Enhanced critical magnetic field for monoatomic-layer superconductor by Josephson junction steps

Fumikazu Oguro,[1,*] Yudai Sato,[1,*] Kanta Asakawa,[1,2] Masahiro Haze,[1] and Yukio Hasegawa[1,†]
[1]*The Institute for Solid State Physics, The University of Tokyo 5-1-5, Kashiwa-no-ha, Kashiwa 277-0882, Japan*
[2]*Department of Applied Physics, Tokyo University of Agriculture and Technology, 2-24-16, Nakacho, Koganei, Tokyo 184-8588, Japan*

(Received 29 October 2020; revised 27 January 2021; accepted 27 January 2021; published 9 February 2021)

We have studied the monoatomic-layer superconductors formed on semiconducting substrates and investigated the role of steps in superconducting properties. In the present study we found that the steps of the Si(111)-$\sqrt{3}\times\sqrt{43}$ Pb reconstructed structure significantly disrupt the electronic states of the superconducting atomic layer and hold Josephson-like vortices under the out-of-plane magnetic field. Because of the strong decoupling, narrow terraces whose width is less than three times the coherence length behave like superconducting nano stripes and exhibit large critical field against the out-of-plane magnetic field. Since monolayer superconductors are intrinsically strong against in-plane magnetic field, superconducting materials highly tolerant against magnetic fields in all directions might be tailored by controlling the step arrangement in the atomic-layer superconductors.

DOI: 10.1103/PhysRevB.103.085416

I. INTRODUCTION

In a usual superconductor, electrons that have opposite momentum are bound to form a Cooper pair, and the pairs condense into a single quantum state to contribute to nondissipative current. Under magnetic fields, the pairs lose their stability as the field exerts forces that unbalance the electrons' orbital momenta. Since breaking the pairs costs an energy, however, superconductivity survives up to a certain amount of magnetic field, called critical magnetic field. Enhancing the robustness against magnetic field is technically important, for instance, for generating high magnetic fields. In the case of thin films, superconductivity is naturally robust against the in-plane magnetic field because the above-mentioned orbital breaking mechanism is suppressed due to geometrical limitation of the electron orbitals. It would therefore be an impact if one finds approaches that make them robust against magnetic fields in other directions.

Here we focus on highly crystalline monoatomic-layer (ML) superconductors formed on a semiconducting substrate [1–8]. The ultimately thin superconducting materials were first discovered on reconstructed structures of Pb and In MLs deposited on Si(111) substrates; on these surfaces the superconducting gaps and vortices were observed using scanning tunneling microscopy and spectroscopy (STM/S) [1]. The presence of the dissipationless current was subsequently confirmed by surface transport measurements [2,3]. As one of the atomically thin superconductors [7,8], their properties intrinsic to two dimensionality and the proximity effect through atomically abrupt interfaces [9–11] have been extensively investigated.

On the surface of semiconducting substrates, monoatomic-height steps exist ubiquitously, and their presence affects the properties of the ML superconductors formed on them. Disrupting the periodical atomic arrangement, the steps usually weaken the coupling of the electronic states of the neighboring terraces [12]. Curiously, roles of the steps on the ML superconductors depend strongly on the system [2,4,5]. In the case of striped-incommensurate (SIC) phase of ML Pb/Si(111), for instance, standard Abrikosov vortices are pinned at step edges with their round shape remaining. In the case of the $\sqrt{7}\times\sqrt{3}$ phase, which is another ML Pb/Si(111) superconducting phase with the Pb coverage of 1.20 ML, slightly less than that of SIC (1.3 ML), the shape of the vortices trapped at steps are elongated along the step direction [4]. The elongated shape is due to reduced critical current density across the steps, indicating a certain degree of decoupling and weakened superconducting link there [4,5]. The elongated vortices are often called a mixed Abrikosov-Josephson vortex [13]. On the $\sqrt{7}\times\sqrt{3}$ phase of ML In/Si(111), the vortex elongation is further extended to form a Josephson vortex along the steps [5], implying significant decoupling there.

In the present study we utilized a ML superconductor whose steps' decoupling is strong enough to form a Josephson-like vortex and to partition the superconducting layer into narrow stripes. When the dimension of narrow stripes is comparable or smaller than the coherence length, superconductivity becomes robust against the magnetic field applied perpendicular to the short dimension because of the suppressed orbital pair breaking. Similar enhancement of the critical field due to small sizes was already achieved by the fabrication of nanosize superconducting island structures [14] and stripes [15]. Here we demonstrate that the step-partitioned narrow terraces also enhance the critical field against the out-of-plane direction. It should be noted here that even separated by the steps ML superconductors still hold macroscopic supercurrent [2,3], unlike the case of completely separated

*These authors contributed equally to this work.
†hasegawa@issp.u-tokyo.ac.jp

nanoislands [14]. Since the distribution of steps can be tailored using techniques established in surface science, the present work opens a path to design and fabricate unique superconducting thin films tolerant to magnetic fields in all directions.

II. EXPERIMENT

We investigated superconductivity using STM. All STM and tunneling conductance measurements were performed at 0.4 K with a ^{3}He-cooled ultrahigh vacuum low-temperature STM (Unisoku USM-1300 with a Nanonis controller) equipped with a superconducting magnet that generates an out-of-plane magnetic field up to 7 T. Tunneling conductance and its spectra were measured in a standard lock-in method using the modulation amplitude and frequency of 0.1 mV and 971 Hz, respectively.

As a sample we used $\sqrt{3}\times\sqrt{43}$ reconstructed phase; one of the "Devil's staircase" phases of the Pb/Si(111) system [16]. The phase was formed by the deposition of 1.5 ML Pb on the Si(111) substrate (As doped, 1–3 mΩ cm) at room temperature and subsequent annealing at 673 K for 120 s. During the postannealing deposited Pb atoms gradually desorb from the substrate, and by tuning the annealing temperature and time, the Pb coverage can be controlled from the SIC phase (1.3 ML) to $\sqrt{3}\times\sqrt{7}$ phase (1.20 ML). Both SIC and $\sqrt{3}\times\sqrt{43}$ (1.23 ML) phases are a mixed phase of local $\sqrt{3}\times\sqrt{3}$ and $\sqrt{3}\times\sqrt{7}$ atomic structures.

III. RESULTS AND DISCUSSION

An STM image taken on the $\sqrt{3}\times\sqrt{43}$ phase is presented in Fig. 1(a). Stripe patterns running along the $[11\bar{2}]$ direction of the substrate are observed. The narrow and wide spacings between the stripes correspond to that of $\sqrt{3}\times\sqrt{3}$ and $\sqrt{3}\times\sqrt{7}$ Pb/Si(111) structures, respectively, indicating that the reconstructed structure is a periodically mixed phase of the two local structures. A tunneling spectrum taken on the phase presented in Fig. 1(b) shows a superconducting gap. From the fitting with the Dynes function [17], whose curve is drawn with a red line in the figure, we found the gap is 0.28 meV, which is close to that of other ML Pb-induced phases: the SIC phase (0.35 meV) and the $\sqrt{3}\times\sqrt{7}$ phase (0.28 meV) [1].

The tip temperature (1.19 K) estimated from the Dynes fitting is significantly higher than the actual one. It is indeed due to broadening of the spectrum; the coherence peaks are lower and broader, and more density of states (DOS) inside the gap near the peaks than those expected from the Bardeen-Cooper-Schrieffer (BCS) function. The broadening, that is, deviation from the BCS function, is partly due to experimental noise. We, however, observed significant broadening or deviation from BCS on monolayer superconductors more than thicker films, suggesting the broadening is intrinsic to the ultimately thin superconductors. According to the Anderson theorem, conventional *s*-wave superconductivity is tolerant against time-reversal invariant disorder. Such disorder, however, may break the two-dimensional superconductivity through the disorder-induced localization and phase fluctuation [4,7,8]. A broken component of triplet superconductivity, which is expected on noncentrosymmetric systems

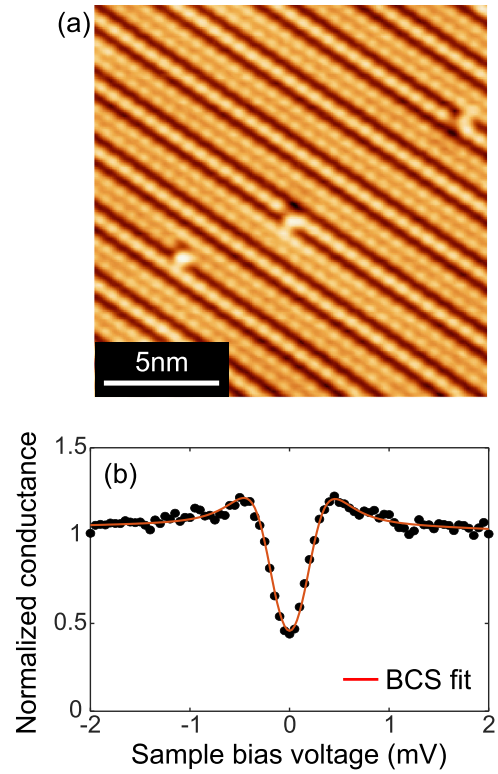

FIG. 1. Atomically resolved STM image of $\sqrt{3}\times\sqrt{43}$ structure (sample bias voltage $V_s = 1$V, set tunneling current $I_t = 100$ pA, 17×17 nm^2). (b) Tunneling conductance (dI/dV) spectrum taken on the structure. The tip height was stabilized with the tunneling condition of $V_s = 10$ mV and $I_t = 200$ pA, and the measured conductance was normalized with the tip-stabilizing conductance (20 nS). The red line shows a fitted Dynes function whose parameters are 0.28 mV, 0.044 mV, and 1.19 K for a superconducting gap, the pair-breaking factor, and the tip temperature, respectively.

including monolayer superconductors formed on a substrate, may also contribute to the broadening [4].

Figure 2(a) shows an STM image taken in a wider area (995×995 nm^2). The whole surface is covered with the $\sqrt{3}\times\sqrt{43}$ phase including the areas close to the step edges, as shown in zoomed images presented in Figs. 2(b)–2(d). The zoomed images also show domain structure; in each domain the $\sqrt{3}\times\sqrt{43}$ stripes run along one of the three equivalent $\langle 11\bar{2}\rangle$ directions. In the same area as Fig. 2(a), we have taken spatial mappings of tunneling conductance at zero bias voltage (ZBC: zero bias conductance), under various out-of-plane magnetic fields. The ZBC value corresponds to the minimum conductance in the superconducting gap, and therefore, a good measure of the breaking of superconductivity in the area just below the tip [14,18]. Figures 3(b)–3(h) show the obtained ZBC mappings. The amount of the magnetic field ranges from 0 to 400 mT. The ZBC mapping taken under zero field [Fig. 3(b)] demonstrates almost uniform distribution of the deep gaps (low ZBC value) over the entire surface, indicting mostly uniform superconductivity including the areas close to the steps and the domain boundaries. The steps do not locally break the superconductivity of the ML Pb structure.

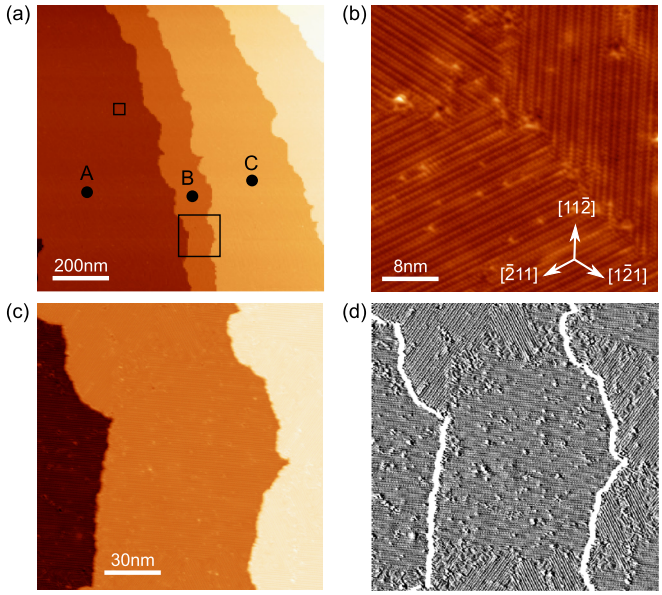

FIG. 2. STM images of the $\sqrt{3}\times\sqrt{43}$ structure taken in wider areas. (a) $995 \times 995\,\mathrm{nm}^2$, $V_s = 10\,\mathrm{mV}$, $I_t = 400\,\mathrm{pA}$, marked A, B, and C, indicate the sites on which the tunneling spectra presented in Fig. 4 were taken. (b), (c) Zoomed STM images taken in the small and large squares depicted in (a), respectively. (b) $V_s = 10$ mV, $I_t = 40$ pA, $40 \times 40\,\mathrm{nm}^2$; (c) $V_s = 80\,\mathrm{mV}$, $I_t = 40\,\mathrm{pA}$, $150 \times 150\,\mathrm{nm}^2$. (d) Derivative $[dh(x, y)/dx]$ image of (c), where $h(x, y)$ is the height at (x, y), to reveal detailed structures.

This is same as the cases of the Pb-induced SIC phase [4] and $\sqrt{7}\times\sqrt{3}$ In/Si(111) structure [5].

When the out-of-plane magnetic fields of 30–100 mT [Figs. 3(c)–3(f)] are applied, several protrusions of high-ZBC (yellow) area are observed. The diameter of the protrusion is ∼100 nm. The number of the protrusions increases with the magnetic field, and the ZBC value at the center of the protrusions is almost same as the ZBC measured at high magnetic fields [e.g., 400 mT of Fig. 3(h)]. These features clearly indicate that the observed protrusions are vortices. In fact, the shape of the vortices observed in wide terraces is not perfectly circular and not well defined, compared with the ones observed on SIC phase [4] and $\sqrt{7}\times\sqrt{3}$-In/Si(111) [5], somehow resembling those of $\sqrt{3}\times\sqrt{7}$ Pb [4]. The blur shape could be due to phase fluctuation induced by disorder such as defects and domain boundaries, and/or thermal/quantum fluctuations [4].

We noticed in the mapping of 30 and 100 mT [Figs. 3(c)–3(f)] that the vortices are formed only inside of wide terraces, apparently repelled from the step edges. In a narrow terrace that is found vertically long around the center of the images, no vortices are observed. Similar vortex repelling from the step edges was also observed on the $\sqrt{7}\times\sqrt{3}$-In/Si(111) ML superconductor, and it was explained with the presence of Josephson vortices at the step edges [5]. A Josephson vortex, formed at a Josephson junction, exhibits an extended core along the junction with suppressed breaking of superconductivity [5]. With the reduced DOS, Josephson vortices appear dark (low) along the step edges in ZBC mappings. Since all the vortices including Josephson vortices interact repulsively with each other, the conventional Abrikosov vortices are repelled apparently from the step edges due to the presence of Josephson vortices there.

In the case of the indium-covered superconductor [5], the decoupling strength of the ML electronic states across the step edges varies significantly depending on the local atomic structure near the step edges. Because of the variation, various types of the vortices are observed around step

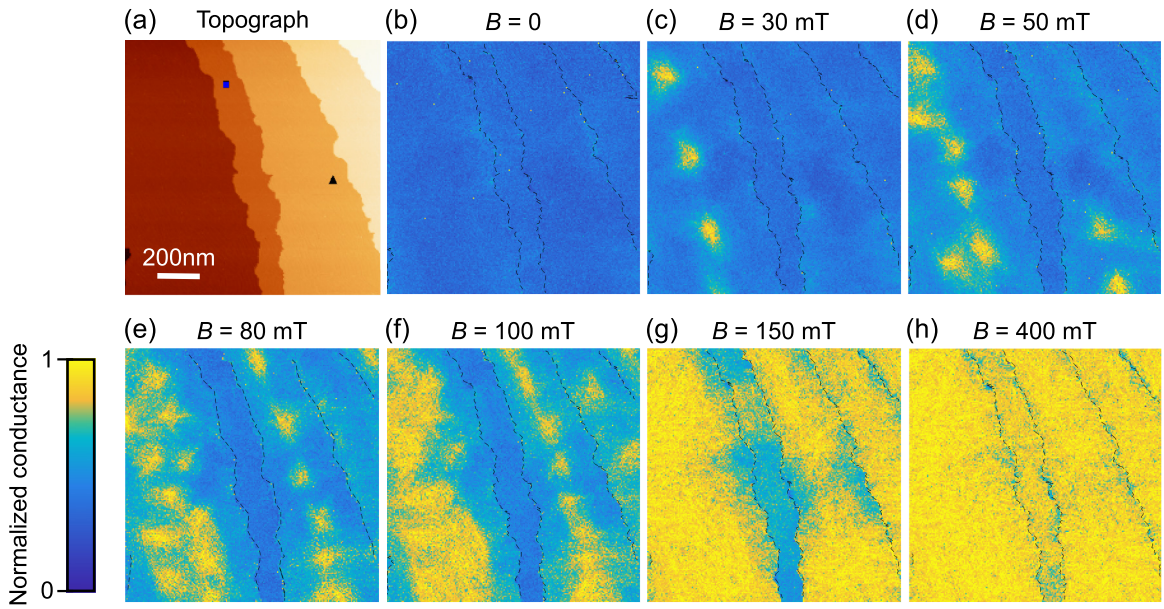

FIG. 3. (a) STM image of the $\sqrt{3}\times\sqrt{43}$ phase of Pb/Si(111) [same as Fig. 2(a)]. (b)–(h) ZBC mappings in the same area as (a) taken under the out-of-plane magnetic field of 0, 30, 50, 80, 100, 150, and 400 mT, respectively. The location of step edges are drawn with fine black dashed lines. The tip stabilization condition is $V_s = 10$ mV and $I_t = 400$ pA. All the ZBC values are normalized by the normal conductance (40 nS).

edges; bright (high ZBC) round one (Abrikosov vortex), intermediate oval one trapped at the step edges (Abrikosov-Josephson vortex) [13], and a dark one extended along a step edge (Josephson vortex) [5]. In our case of the $\sqrt{3}\times\sqrt{43}$ structure, on the other hand, presumably because of uniform atomic structure proximate to the step edges, the step edges remain dark; no trapped vortices are apparently found there.

Actually in the ZBC mapping taken at 30 mT [Fig. 3(c)], there are several areas around step edges whose ZBC is slightly larger than that of surrounding terraces. Since the number of such high-ZBC areas plus vortices is roughly consistent with the one expected from the applied magnetic field (15 vortices in the view), we identify these high-ZBC areas as a vortex with strongly (but not perfectly) suppressed breaking of superconductivity extended along the step edges [5], that is, Abrikosov-Josephson vortex [4,13]. Since the height in ZBC on the vortices is only 10% of the normal conductance, the contribution of a Josephson vortex is dominant [5], and therefore we call them a Josephson-like vortex hereafter in this paper. These findings lead us to conclude that all the step edges of the $\sqrt{3}\times\sqrt{43}$ phase always work as a Josephson junction and significantly decouple the superconducting electronic states.

In fact, similar high-ZBC areas are also observed in the ZBC mapping taken under 0 T [Fig. 3(b)]. Since the ZBC height and the shape are similar with the Josephson-like vortices observed at 30 mT, they are also presumably Josephson-like vortices trapped at step edges [5] formed during magnetic sweeps prior to the measurement.

With the increment in the applied magnetic field, the number of vortices increases. The vortices are squeezed within wide terraces, gradually losing their boundaries [13,19–21]. In addition, the amount of ZBC behind the vortices gradually increases. At 150 mT [Fig. 3(g)], the vortices almost lose their contrast with the background, which signals saturation of ZBC. Figure 4 shows superconducting gaps taken on the three sites marked in the STM image of Fig. 2(a) under various out-of-plane magnetic fields. Those spectra clearly indicate that the increment in ZBC observed in the ZBC mappings is indeed due to the shallowing of the superconducting gap, that is, due to the recovery of DOS by the Cooper pair breaking. Strikingly, in the narrow terrace, ZBC is still low under the magnetic field of 150 mT [Fig. 3(g)], demonstrating suppression of the superconductivity breaking there. The comparison of the tunneling spectra (Fig. 4) taken under 100 mT also supports for the suppressed breaking; the spectrum taken in narrow terrace (Site B) at 100 mT (depicted with blue dots) is still deep. Meanwhile those taken in wide terraces (Sites A and C) under the same magnetic fields lose the gap significantly. In order to break the superconductivity completely in the narrow terrace, further increase in the magnetic field was required up to 400 mT [Fig. 3(h)]. Under 400 mT, all the area reached the saturated ZBC value, and the superconductivity is broken in the whole area. The spatially resolved ZBC evolution presented in Fig. 3 as well as the tunneling spectra shown in Fig. 4 clearly demonstrates that the field that makes ZBC saturated, namely critical magnetic field, is larger in the narrow terrace than the wide terraces. Figure 5 shows other sets of STM image and the corresponding ZBC

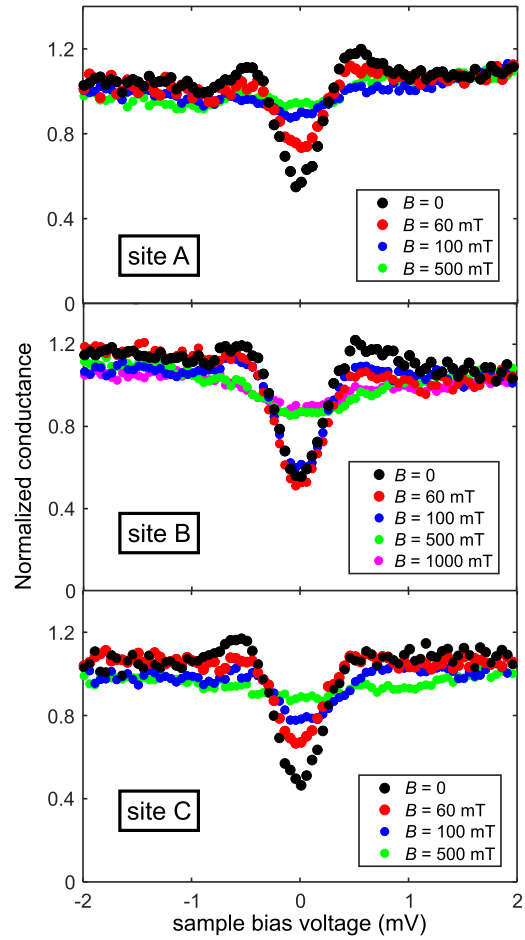

FIG. 4. Tunneling spectra taken on the sites marked in the STM image of Fig. 2(a) under the out-of-plane magnetic field of 0, 60, 100, 500, and 1000 mT. The tip stabilization condition is $V_s = 10$ mV and $I_t = 400$ pA. All the measured conductance values are normalized by the normal conductance (40 nS).

mapping taken on the same $\sqrt{3}\times\sqrt{43}$ phase under the out-of-plane magnetic field. These images also demonstrate deep superconducting gaps and suppressed breaking of superconductivity in narrow terraces.

The behavior of Josephson-like vortices is also different in the narrow terrace. The high-ZBC area due to a Josephson-like vortices usually spreads into both terraces of the step edge that the vortex sits on [5]. In the ZBC mappings of 30 and 50 mT [Figs. 3(c) and 3(d)], Josephson-like vortices found on the step edge in the right side of the probed area, which separates two wide terraces, spread into both sides. In the case of the narrow terrace, however, the high-ZBC area is observed only on the wide-terrace side of the step edge. We presume that these peculiar vortex behaviors are also related with the terrace width, and could be related to the presence of the other Josephson vortex across the narrow terrace.

As already mentioned, there are some defects and domain boundaries on terraces. As far as we observed in STM images, one of which is shown in Fig. 2(c), however, we did not find any differences in the defect density or distribution among the terraces including narrow ones. It is thus unlikely that the narrow terrace has electronic structure different from that of

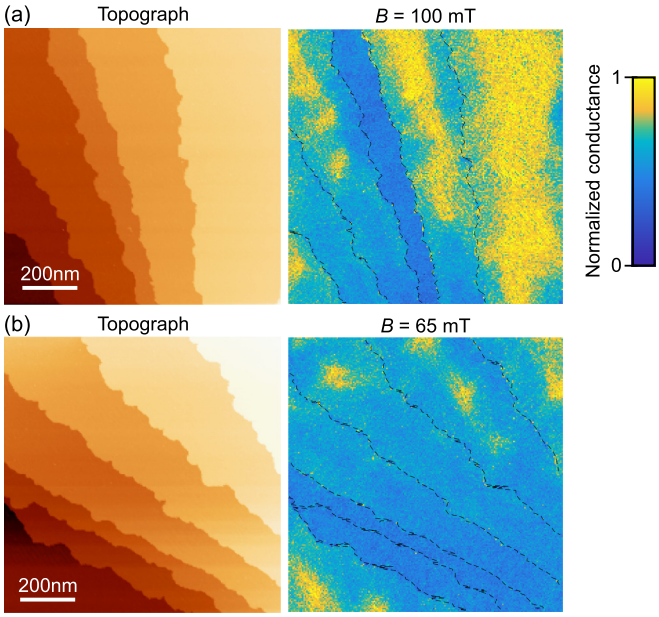

FIG. 5. Two sets of STM topographic image and corresponding ZBC mapping under out-of-plane magnetic field taken on the $\sqrt{3}\times\sqrt{43}$ phase to demonstrate suppressed breaking of superconductivity in narrow terraces. The size of the images is $995 \times 995\,\mathrm{nm}^2$, same as that of Fig. 2(a). On the ZBC mappings, the location of step edges are drawn with fine black dashed lines. The tip stabilization condition is $V_s = 10\,\mathrm{mV}$ and $I_t = 400\,\mathrm{pA}$. All the ZBC values are normalized by the normal conductance (40 nS).

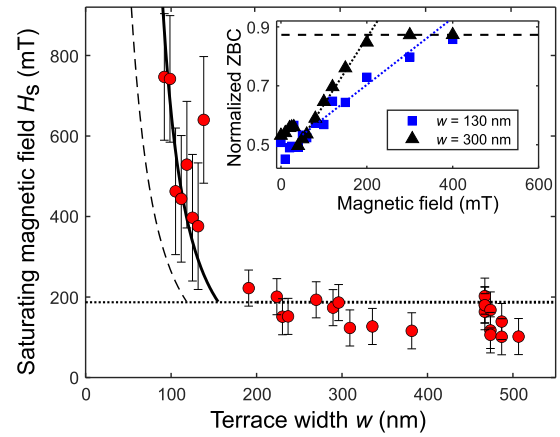

FIG. 6. Plot of saturating magnetic field H_s as a function of the terrace width w. Solid and dashed lines indicate an equation of $H_{c2} = \sqrt{12}\phi_0/2\pi\xi(w - w_0)$ with $w_0 = 58$ and 0 nm, respectively. Dotted horizontal bar indicates the nominal upper critical field for wide terraces. The inset shows a plot of the ZBC evolution, that is, normalized ZBC as a function of the applied out-of-plane magnetic field. Data sets depicted with blue squares and black triangles are taken on terraces whose widths are 130 and 300 nm, respectively, as marked with the corresponding symbols on the STM image of Fig. 3(a). ZBC values are linearly fitted with the dotted lines, and the dashed bar indicates the saturated value of ZBC measured in 400 mT. From the intersection of the two lines, the saturation field H_s was obtained.

wider ones. Whereas we call it a narrow terrace, the terrace width is more than 100 nm, wide enough to eliminate the effect of quantum interference due to the laterally confined electronic states within the terrace.

In Fig. 4, one may notice that the tunneling spectra taken at high magnetic field (500 and 1000 mT) are not completely flat, showing a shallow dip around the Fermi energy. This feature, often observed on ML metals, is explained with dynamical Coulomb blockade [22]. Since the dependence of its shape and depth on magnetic fields is negligibly small, we can safely distinguish it with superconducting gaps. Due to the dip feature, the ZBC values do not reach the normal conductance (conductance outside of the superconducting gap), which is used for the normalization in Fig. 4, but the saturation of ZBC by the magnetic field definitely indicates complete breaking of superconductivity.

From the evolution of ZBC images with the applied magnetic field we can estimate the value of the critical field (H_{c2}) at each site. Here, using the obtained ZBC mappings we investigated how the critical field depends on the terrace width in a quantitative manner. For the analysis we first estimated H_{c2} at various sites by measuring the amount of the out-of-plane magnetic field H_s that saturates ZBC. The inset of Fig. 6 shows two typical ZBC evolutions measured at the sites marked with the corresponding symbols in the STM image of Fig. 3(a). The saturating field was determined from an intersection of an extrapolated linear line with a horizontal dashed bar of the saturated ZBC [1]. As mentioned above, the saturated ZBC was evaluated from the ZBC taken at high magnetic field (400 mT), and it is smaller than the normal conductance (that is, the normalized conductance is <1) because of dynamical Coulomb blockade, as already mentioned. In Fig. 6, the obtained H_s was plotted as a function of the terrace width w.

When the terrace width is significantly large compared with the coherence length, the critical field is described with the coherence length ξ as $H_{c2} = \phi_0/2\pi\xi^2$, where ϕ_0 is magnetic flux quantum ($= h/2e$ with the Planck constant h and the electron charge e), and thus should not depend on the terrace width. On the terraces wider than 200 nm, there are several data whose saturating field is smaller than other sites of similar or larger terrace width. These are artifacts due to the coverage of the measured site with vortices during the evolution. Since vortices increase ZBC, the sites covered with vortices tend to reach the saturated ZBC at a magnetic field smaller than the critical field. We thus omit these sites from further analysis. From the maximum saturating magnetic field taken on terraces significantly wider than the vortex size, we estimated the nominal critical field is 190 mT (dotted horizontal bar in Fig. 6), and evaluated the coherence length ξ as 42 nm from the equation of H_{c2}. The evaluated coherence length is consistent with the size of the vortices ($\sim$50 nm in radius). It is also comparable with those of other Pb ML superconducting phases; $\sqrt{7}\times\sqrt{3}$ (45 nm) and SIC ($\sim$50 nm) [1,4].

The plot in Fig. 6 exhibits a crossover in H_{c2} around the terrace width of 200 nm. For the terraces wider than 200 nm the critical field is the nominal value, and for the terrace narrower than 200 nm it increases steeply with the reduction in the terrace width. The steep increase in

H_{c2} for the narrow terraces can be explained with the Ginzburg-Landau (GL) equation. According to the linearized GL equation, the critical field H_{c2} of superconducting stripes whose width is narrow enough to exhibit uniform order parameter is given by a formula of $H_{c2} = \sqrt{12}\phi_0/2\pi\xi w$ (Ref. [23]). We expected our critical fields measured on terraces whose width is less than 200 nm are also explained with the formula. As shown in the plot, however, H_{c2} of our step-confined terraces was markedly larger than the formula (dashed line in the plot). In order to explain the anomalous results, we temporarily introduced a width-reduction factor w_0 in the formula as $H_{c2} = \sqrt{12}\phi_0/2\pi\xi(w - w_0)$, and found good agreements with $w_0 = 58$ nm (thick line).

The effective reduction in the terrace width is obviously due to the presence of neighboring terraces, but theoretical calculation based on the GL equation including neighboring terraces that are separated with Josephson junction cannot explain the reduced width. The width reduction could, then, be due to the presence of Josephson-like vortices at the step edges. Since their superconducting behavior is different, the area of the vortices should be removed from the GL analysis. As they sit along the step edges, this implies removing the width of ξ for each edge, giving the correct qualitative behavior with the proposed GL formulation. We need further theoretical analysis for understanding the mechanism. H_{c2} of terraces narrower than w_0 is also curious as our formula does not provide a realistic answer. This should also be investigated in the near future. Nevertheless our present analysis leads us to conclude that the step confinement makes the superconductor tolerant against the out-of-plane magnetic field. It should be noted here that since the steps work as a Josephson junction, the superconductivity is not totally disconnected; coherent supercurrent flows across the steps [2], which is an important aspect for practical applications.

In this study, we found that H_{c2} in narrow terraces of the $\sqrt{3}\times\sqrt{43}$ phase, one of the Pb-induced reconstructed structure on the Si(111) substrate, is enhanced against the out-of-plane magnetic field. With expected high H_{c2} against the in-plane magnetic field, we believe that the step-confined 2D superconductor should exhibit high H_{c2} in all directions of magnetic fields, which should be confirmed in future work. The H_{c2} enhancement by narrow terraces, however, does not occur in all the ML superconductors because of different roles of steps on the surface 2D electronic states. Whether H_{c2} is enhanced or not depends on the decoupling strength of the electronic states by step edges. As is already mentioned, on the SIC phase the steps work as a pinning center for vortices [4], implying weak decoupling between the neighboring terraces. In the case of the $\sqrt{7}\times\sqrt{3}$ phase of Pb/Si(111), oval vortices are found along the step edges, indicating intermediate decoupling [4]. In either case, the H_{c2} enhancement does not occur. On the other hand, on the $\sqrt{3}\times\sqrt{43}$ systems all the step edges strongly decouple the electronic states of the neighboring terraces and contribute to the enhancement of H_{c2}. For ML superconductors, the energy level of the metallic 2D states that host superconductivity is within the band gap of the semiconducting substrate, and therefore the amplitude of the 2D states' wave function decays quickly into the substrate. The decoupling strength may be related with the decay length of the 2D states and its relation with the step height. For the states with short decay length, the 2D electronic states localized on the surface are significantly decoupled by the step edges. For the deep-decaying states, on the other hand, the steps does not affect the connection of the electronic states so much. Since the decay length is presumably dependent on the energy level of the states within the gap of the substrate, a systematic study combining photoemission spectroscopy to probe the energy level of the states with STM will unveil the relation of the surface 2D electronic states and the tolerance of superconductivity against magnetic fields.

IV. CONCLUSION

We found that the steps of the superconducting ML-Pb $\sqrt{3}\times\sqrt{43}$ phase, which hold Josephson-like vortices under the out-of-plane magnetic field, significantly disrupt the superconducting electronic states. Due to the strong decoupling, narrow terraces behave like superconducting nanostripes and exhibit large critical field against the out-of-plane magnetic field. Since ML superconductors are intrinsically robust against in-plane magnetic field, superconducting thin films highly tolerant against magnetic fields in all directions could be tailored by controlling the step configuration of the atomic-layer superconductor. The present work opens a path to design and fabricate unique superconducting materials by utilizing the peculiar roles of step edges.

ACKNOWLEDGMENTS

We thank T. Uchihashi and M. Milosevic for fruitful discussions. This work was partially supported by Grants-in-Aid for Scientific Research from the Japan Society for the Promotion of Science (Grants No. JP16H02109, No. JP18K19013, and No. JP19H00859).

[1] T. Zhang, P. Cheng, W.-J. Li, Y.-J. Sun, G. Wang, X.-G. Zhu, K. He, L. Wang, X. Ma, X. Chen, Y. Wang, Y. Liu, H.-Q. Lin, J.-F. Jia, and Q.-K. Xue, Nat. Phys. **6**, 104 (2010).

[2] T. Uchihashi, P. Mishra, M. Aono, and T. Nakayama, Phys. Rev. Lett. **107**, 207001(2011).

[3] M. Yamada, T. Hirahara, and S. Hasegawa, Phys. Rev. Lett. **110**, 237001 (2013).

[4] C. Brun, T. Cren, V. Cherkez, F. Debontridder, S. Pons, D. Fokin, M. C. Tringides, S. Bozhko, L. B. Ioffe, B. L. Altshuler, and D. Roditchev, Nat. Phys. **10**, 444 (2014).

[5] S. Yoshizawa, H. Kim, T. Kawakami, Y. Nagai, T. Nakayama, X. Hu, Y. Hasegawa, and T. Uchihashi, Phys. Rev. Lett. **113**, 247004 (2014).

[6] T. Nakamura, H. Kim, S. Ichinokura, A. Takayama, A. V. Zotov, A. A. Saranin, Y. Hasegawa, and S. Hasegawa, Phys. Rev. B **98**, 134505 (2018).

[7] T. Uchihashi, Supercond. Sci. Technol. **30**, 013002 (2017).

[8] C. Brun, T. Cren, and D. Roditchev, Supercond. Sci. Technol. **30**, 013003 (2017).

[9] J. Kim, V. Chua, G. A. Fiete, H. Nam, A. H. MacDonald, and C.-K. Shih, Nat. Phys. **8**, 464 (2012).
[10] V. Cherkez, J. C. Cuevas, C. Brun, T. Cren, G. Ménard, F. Debontridder, V. S. Stolyarov, and D. Roditchev, Phys. Rev. X **4**, 011033 (2014).
[11] H. Kim, S.-Z. Lin, M. J. Graf, Y. Miyata, Y. Nagai, T. Kato, and Y. Hasegawa, Phys. Rev. Lett. **117**, 116802 (2016).
[12] M. Ono, Y. Nishigata, T. Nishio, T. Eguchi, and Y. Hasegawa, Phys. Rev. Lett. **96**, 016801 (2006).
[13] A. Gurevich, M. S. Rzchowski, G. Daniels, S. Patnaik, B. M. Hinaus, F. Carillo, F. Tafuri, and D. C. Larbalestier, Phys. Rev. Lett. **88**, 097001 (2002).
[14] T. Nishio, T. An, A. Nomura, K. Miyachi, T. Eguchi, H. Sakata, S. Lin, N. Hayashi, N. Nakai, M. Machida, and Y. Hasegawa, Phys. Rev. Lett. **101**, 167001 (2008).
[15] H. Nam, H. Chen, P. W. Adams, S.-Y. Guan, T.-M. Chuang, C.-S. Chang, A. H. MacDonald, and C.-K. Shih, Nat. Commun. **9**, 5431 (2018).
[16] M. Hupalo, J. Schmalian, and M. C. Tringides, Phys. Rev. Lett. **90**, 216106 (2003).
[17] R. C. Dynes, J. P. Garno, G. B. Hertel, and T. P. Orlando, Phys. Rev. Lett. **53**, 2437, (1984).
[18] D. Eom, S. Qin, M.-Y. Chou, and C. K. Shih, Phys. Rev. Lett. **96**, 027005 (2006).
[19] T. Cren, D. Fokin, F. Debontridder, V. Dubost, and D. Roditchev, Phys. Rev. Lett. **102**, 127005 (2009).
[20] T. Cren, L. Serrier-Garcia, F. Debontridder, and D. Roditchev, Phys. Rev. Lett. **107**, 097202 (2011).
[21] T. Tominaga, T. Sakamoto, H. Kim, T. Nishio, T. Eguchi, and Y. Hasegawa, Phys. Rev. B **87**, 195434 (2013).
[22] L. Serrier-Garcia, J. C. Cuevas, T. Cren, C. Brun, V. Cherkez, F. Debontridder, D. Fokin, F. S. Bergeret, and D. Roditchev, Phys. Rev. Lett. **110**, 157003 (2013).
[23] M. Tinkham, *Introduction to Superconductivity, 2nd Edition* (McGrow-Hill Book Co., New York, 1975).